Photochemical & Photobiological Sciences

Accepted Manuscript

This is an *Accepted Manuscript*, which has been through the Royal Society of Chemistry peer review process and has been accepted for publication.

Accepted Manuscripts are published online shortly after acceptance, before technical editing, formatting and proof reading. Using this free service, authors can make their results available to the community, in citable form, before we publish the edited article. We will replace this *Accepted Manuscript* with the edited and formatted *Advance Article* as soon as it is available.

You can find more information about *Accepted Manuscripts* in the Information for Authors.

Please note that technical editing may introduce minor changes to the text and/or graphics, which may alter content. The journal's standard Terms & Conditions and the Ethical guidelines still apply. In no event shall the Royal Society of Chemistry be held responsible for any errors or omissions in this *Accepted Manuscript* or any consequences arising from the use of any information it contains.

ROYAL SOCIETY OF CHEMISTRY

www.rsc.org/pps

Photochemical & Photobiological Science

RSCPublishing

ARTICLE

The photophysics of LOV-based fluorescent proteins – new tools for cell biology

Cite this: DOI: 10.1039/x0xx00000x

Received ooth January 2012,
Accepted ooth January 2012

DOI: 10.1039/x0xx00000x

www.rsc.org/

Marcus Wingen[a], Janko Potzkei[a], Stephan Endres[a], Giorgia Casini[b], Christian Rupprecht[a], Christoph Fahlke[b], Ulrich Krauss[a], Karl-Erich Jaeger[a], Thomas Drepper[*a], and Thomas Gensch[*b]

LOV-based fluorescent proteins (FPs) are an alternative class of fluorescent reporters with unique properties which complement the well-established proteins of the GFP family. One of the most important features of LOV-based FPs is the independence of molecular oxygen for the development of their specific fluorescence. Furthermore, they are characterized by their small size and rapid signal development. Over the last few years, a number of different bacterial and plant LOV-based fluorescent proteins such as FbFP, iLOV and miniSOG have been developed and optimized. In this report, we comparatively characterized the photophysical properties of nine different LOV-based fluorescent proteins including the excitation and emission maxima, the extinction coefficient, the fluorescence quantum yield, the average fluorescence lifetime and the photostability. The unified characterization of the LOV-based FPs provides a useful guide to applying them as *in vivo* tools for quantitative analyses and biological imaging.

Introduction

The analysis of gene expression as well as the localization, movement, and interaction of the corresponding gene products in living cells and tissues enables deep insights into complex cellular structures and dynamics. A detailed understanding of such biological processes in the cellular context, in turn, is strictly dependent on the ability to visualize and monitor dynamic events *in vivo* with high spatial and temporal resolution. To this end, fluorescent reporter proteins developed as variable and popular *in vivo* research tools in cell biology [1-5], mainly because of the versatile applicability for fluorescent imaging and quantitative analyses of the green fluorescent protein (GFP) and its sophisticated variants. However, the use of GFP-like *in vivo* reporters is restricted by various environmental and cellular factors impeding either chromophore formation or fluorescence activity. Here the most prominent example is the incomplete autocatalytic synthesis of the chromophore in the absence of molecular oxygen, leading to the accumulation of inactive, non-fluorescing reporter proteins [6, 7]. To conquer this limitation, alternative fluorescent proteins that are based on blue-light photoreceptors of the LOV (light oxygen voltage) family, have been developed recently [8-11]. These cyan-green fluorescing proteins bind flavin mononucleotide (FMN) as the chromophore and are either derived from bacterial photoreceptors (FMN-binding fluorescent proteins; FbFP [8]) or are derivatives of the *Arabidopsis thaliana* phototropin 2 LOV2 domain (iLOV, miniSOG; [9, 12]). In contrast to all members of the GFP family, this novel class of LOV-based FPs develops the corresponding fluorescence signal under both, aerobic and anaerobic conditions [8, 13, 14]. This unique property renders them valuable for *in vivo* applications where molecular oxygen is limited; such as the analysis of microbial pathogenesis, hypoxia induced inflammatory processes, tumor pathophysiology and microbial fermentation as well as for the monitoring and optimization of bioremediation and bacterial production processes (e.g. [15, 16-25]). Since the first description in 2007 [8] LOV-based FPs were successfully applied in different hypoxic environments [13, 14, 26-29]. Recently, a Förster resonance energy transfer (FRET) - based, genetically encoded biosensor called FluBO has been developed and characterized [30]. The oxygen biosensor consists of a FbFP as oxygen-independent FRET-donor domain and EYFP as oxygen-dependent FRET-acceptor domain. Due to the selective oxygen-dependency of EYFP chromophore formation, FluBO enables the ratiometric determination of intracellular oxygen levels in living cells *via* the O_2-dependent change of FluBOs FRET efficiency.

Additionally, LOV-based FPs are characterized by their notable small mass of only ~ 12 – 16 kDa (see table 1), as compared to ~ 27 kDa for members of the GFP family. Therefore, LOV-based FPs could successfully be established within research fields where the size of the fluorescent label is critical. For example, the use of iLOV as alternative fluorescent tag enabled advanced studies of the localization, movement and dynamics of target proteins and viruses [9, 10, 31, 32]. Furthermore, *in vivo* and *in vitro* studies demonstrated that, in contrast to GFP-like proteins, LOV-based reporter proteins rapidly gain their fluorescence-active conformation because of their fast folding kinetics and the spontaneous incorporation of the chromophore [14, 33], thereby enabling their application as real-time reporters. Their rapid assembly as well as the robustness of the fluorescence signal have rendered LOV-based FPs valuable quantitative reporters for biotechnological approaches [33-37].

To further establish LOV-based FPs as alternative fluorescent proteins, some of their biochemical and photophysical properties, including the fluorescence quantum yield, thermal stability and photobleaching susceptibility have been optimized in different studies by directed evolution approaches and site-directed mutagenesis [9, 10, 12, 38, 39] and were subsequently determined with individual techniques. However, quantitative conclusions from spectrometry, cytometry and microscopy data vitally depend on the accurate characterization of their spectral properties that have been obtained under defined and comparable conditions. Within this study we therefore determined the photophysical parameters relevant for fluorescence applications of already known as well as new members (DsFbFP, Pp1FbFP) of the LOV-based FP family. This comprehensive characterization thus builds the prerequisite to accurately use this novel group of fluorescent proteins for analytic methods as well as imaging approaches. Additionally, this data provides a starting point for engineering improved LOV-based FP variants.

Materials and methods

Expression and purification of LOV-based fluorescent proteins

E. coli strain DH5α [40] was used for DNA cloning of the expression vectors encoding the LOV-based fluorescent reporter proteins. *E. coli* strain BL21(DE3) (Novagen, distributed by Merck KGaA, Darmstadt, Germany) was used for expression of the fluorescent proteins. Prior to protein expression and purification, the LOV-based FP-encoding genes were cloned into the *Nde*I and *Xho*I restriction sites of the pRhotHi-2 [41] and pET28a (Novagen, distributed by Merck KGaA, Darmstadt, Germany) expression vectors, respectively.
For gene expression and protein purification, bacterial cells were grown in 1 liter auto-induction terrific broth (TB) medium containing 12 g/l hydrolyzed casein, 24 g/l yeast extract, 9.4 g/l K_2HPO_4, 2.2 g/l KH_2PO_4, (pH 7.2), 4 ml/l glycerol, 0.05 % glucose, 0.2 % lactose in 5 liter shake flasks at 37 °C for 24 hours. All media were supplemented with 50 µg/ml kanamycin to maintain the expression vectors.
The FP variants were purified as His_6-tagged proteins using Ni-NTA metal-ion-exchange-chromatography-superflow-columns (Qiagen, Hilden, Germany), under standard operation conditions as described by the manufacturer. The purified proteins were stored at 4°C in protein storage buffer containing 10mM NaCl, 10mM NaH_2PO_4, pH 8.0.

Isolation and generation of novel LOV-based FP variants

The genes encoding DsFbFP and Pp1FbFP were constructed either by overlap extension PCR or Quik-Change mutagenesis. Plasmids pRhotHi2-DsLOV and pET28a-PpSB1-LOV encompassing the respective LOV photoreceptor genes from *Dinoroseobacter shibae* (DsLOV) [42], and *Pseudomonas putida* (PpSB1-LOV) [43], were used as templates. The photoactive cysteine residue (C72) of DsLOV was replaced by alanine using overlap extension PCR, performed with the primers DsLOV+*NdeI*-up: 5'-GAGTCGCATATGCGCAGACATTATCGCGACCTGAT-3' and DsLOV+*XhoI*-dn: 5'-AATAATCTCGAGGACCGGGTTCTGGGCGCCTGCGAAGAA-3', DsLOV_C72A_up: 5'-CTGGGCCGCAACGCGCGTTTCCTGC-3' and DsLOV_C72A_down: 5'-GCAGGAAACGCGCGTTGCGGCCCAG-3'. The final PCR fragment was hydrolyzed with *Nde*I and *Xho*I and subsequently cloned into the respective sites of the T7 expression vector pET28a. To generate the Pp1FbFP (i.e. PpSB1-LOV C53A) encoding gene, the oligonucleotide primers SB1_C53A_fw: 5'-GATTCTCTACCAGGATGCCCGGTTCCTGCAGGG-3' and SB1_C53A_rev: 5'-CCCTGCAGGAACCGGGCATCCTGGTAGAGAATC-3' were used for Quik-Change PCR. Parental template DNA was hydrolyzed with *DpnI* prior to transformation of the Quikchange-PCR product. The final expression vectors were designated as pET28a-DsFbFP and pET28a-Pp1FbFP.
To improve the photophysical properties of Pp2FbFP (previously designated PpFbFP [8]), point mutations were introduced into the corresponding gene by saturation mutagenesis using overlap extension PCR with degenerated primers.
For Y112 the following primers were used: Y112X5'for: 5'-GAGTTCTTCTGAGCGGGACTCTGG-3', Y112X5'rev: 5'-CTGGATGCCGATNNNGTAGGTCAGC-3', Y112X3'for: 5'-CCAGCTGACCTACNNNATCGGCATCC-3', Y112X3'rev: 5'-CAACTCAGCTTCCTTTCGGGCTTTG-3'. For Q116 the following primers were used: Q116X5'for: 5'-ACGAGTTCTTCTGAGCGGGACTCTGG-3', Q116X5'rev: 5'-TGTGACATCGCGGTGGATGCCGATGTAG-3', Q116X3'for: 5'-CTACTACATCGGCATCNNNCGCGATGTC-3', Q116X3'rev: 5'-GGGCTTTGTTAGCAGCCGGATCTCAG-3'. For the final amplification of the Y112X and Q116X constructs the primers final for: 5'-GGGAATTGTGAGCGGATAAC-3' and final rev: 5'-TTAGCAGCCGGATCTCAG-3' were used. The PCR products were cloned into the pET28a using the *NdeI* and *XhoI* restriction sites. The resulting Pp2FbFP variants were first screened for their *in vivo* fluorescence brightness on agar plates and subsequently characterized in liquid batch cultures in shake flasks. For this, the brightest colonies were picked from the agar plates and cells were grown in 10 ml autoinduction TB medium in 100 ml shake flasks for 24 hours. Subsequently, cells were harvested by centrifugation. Fluorescence spectra (see below), were recorded with 1 ml of cell suspension adjusted to an optical density of 0.5 (λ_{abs} = 580 nm) in 100 mM Tris-HCl, pH 8.0. To identify the underlying mutations of the brightest Pp2FbFP variants, corresponding plasmids have been re-isolated from *E. coli* and FbFP genes were subsequently sequenced (Eurofins MWG Operon, Ebersberg, Germany).

Spectral analysis and fluorometry

The photophysical properties of LOV-based FPs were determined in protein storage buffer (10mM NaCl, 10mM NaH_2PO_4, pH 8.0). To minimize inner filtering and reabsorption effects, all samples were adjusted to a maximum absorption of 0.1 (λ_{abs} = 450 nm).
Absorption spectra were measured using a UV-2450 absorption spectrophotometer (Shimadzu Europa GmbH, Duisburg, Germany). Fluorescence spectra were analyzed using a QuantaMaster 40 fluorescence spectrophotometer (Photon Technology International, Birmingham, NJ, USA).
Fluorescence quantum yields were determined using an integrating sphere in a QuantaMaster 40 fluorescence spectrophotometer at a temperature of 20 ± 2 °C. The extinction coefficient of the proteins at their main absorption maximum in the blue spectral region was determined by measuring the absorption of the protein samples at the respective wavelength

at 20 °C (where the chromophore is bound to the protein) and at 95 °C (where the chromophore is dissociated from the protein). The ratio of both absorption values was then multiplied with the extinction coefficient of free FMN 12,200 $M^{-1}cm^{-1}$ at 450 nm [44] to determine the extinction coefficient of the chromophore in its protein-bound state.

Photobleaching kinetics were recorded in a Cary Eclipse fluorescence spectrophotometer (Agilent Technologies, Santa Clara, Ca, USA) at 20 ± 2 °C. A 700-µl protein sample was filled in a quartz cuvette (0.2 cm × 1 cm × 4 cm) in the sample holder of the spectrophotometer and illuminated by a blue high-power LED (LUXEON Rebel LXML PR01 0425 royalblue (Philips Lumileds, San Jose, Ca, USA); operating current: 350mA; optical power: 180 mW × cm^{-2}; center wavelength: 448 nm) with a 20 mm lens (angle of radiation = 12°), which was placed directly above the cuvette (distance to measured volume in fluorescence spectrometer: ca. 30 mm). Kinetics were recorded with a data interval of 1 second and the first data point below 50% was taken as the bleaching half-time.

The time-resolved detection of the fluorescence intensity decay of all LOV-based FPs and FMN was performed with a Fluotime100 fluorescence spectrophotometer (Picoquant, Berlin, Germany) based on a picoHarp300 unit by using a pulsed diode laser (Laser Picoquant LDH-C440; emission: 440 nm; pulse width: 50 ps; used repetition frequency: 20 MHz) as an excitation source. Fluorescence decay curves as a function of time (t) were measured by time-correlated single-photon counting that enables the determination of fluorescence decay components with fluorescence lifetimes greater than 100 ps [45, 46]. Decay curves were analyzed by iterative reconvolution of the instrument response function, IRF(t), with an exponential model function, M(t), using the FluoFit software (version 4.5.3.0; Picoquant) applying equations 1 and 2:

$$I(t) = IRF(t) \times M(t) \quad (1)$$

$$M(t) = \sum_{i=1}^{n} \left[\alpha_i \times \exp\left(-\frac{t}{\tau_i}\right)\right]; \text{n=1 or 2} \quad (2)$$

τ_i are the characteristic lifetimes and α_i are the respective intensities.

The average lifetime, τ_{flave}, was calculated using equation 3:

$$\tau_{fl,ave} = \frac{\sum_{i=1}^{n}(\alpha_i \times \tau_i)}{\sum_{i=1}^{n}\alpha_i} \quad ; \text{n = 1 or 2} \quad (3)$$

Sequence analysis and modeling of protein structures

Sequence alignments were generated using Clustal omega [47] and analyzed with GeneDoc (http://www.nrbsc.org/gfx/genedoc). Protein structure models were build using the program MODELLER [48] and the known crystal structure of the YtvA LOV domain (PDB ID: 2PR5 [49]) as a template. Models were visualized with UCSF Chimera [50].

Results and discussion

Since the first development of LOV-based FPs [8, 9], several improved variants have been generated [10, 12]. In this work, we thus comparatively analyzed the photophysical properties of BsFbFP and EcFbFP, both engineered from *Bacillus subtilis* YtvA, as well as PpFbFP, a derivative of *Pseudomonas putida* PpSB2-LOV, as bacterial LOV-based FPs. PpFbFP variants Y112L and Q116V were constructed by saturation mutagenesis (details are described in the materials and methods section), and in addition, the plant-LOV based FPs, miniSOG and phiLOV2.1 were further characterized. These fluorescent reporter proteins were derived from the phototropin2 LOV2 domain of *A. thaliana* and were shown to either efficiently generate singlet oxygen upon blue-light irradiation [12] or exhibit improved photostability [10].

To further exploit naturally occurring LOV variants, two novel LOV-based FPs, namely DsFbFP (isolated from the marine α proteobacterium *Dinoroseobacter shibae* [42]) and Pp1FbFP (derived from the *P. putida* LOV protein Pp1SB1-LOV [43, 51]), were created for this study. Both of these two novel FbFPs originate from "short LOV" proteins, a class of LOV receptors that do not possess any fused effector domains. Formation of the non-fluorescing LOV photoadduct during the light-triggered photocycle was prevented by substitution of the cysteine that binds to FMN during the photocycle (DsFbFP: Cys72, Pp1FbFP: Cys53) by an alanine as described previously [8]. To avoid confusion with nomenclature, the first described PpFbFP that is based on the PpSB2-LOV-domain [43], is now designated as Pp2FbFP.

Figure 1 depicts the alignment of the amino acid sequences of nine LOV-based FPs under study. Pp1FbFP and Pp2FbFP show a high sequence identity of 70%. In addition, miniSOG and phiLOV2.1, both derivatives of the LOV 2 domain of *Arabidopsis thaliana* phototropin 2, share a sequence identity of 92%. The typical sequence identities between the here described LOV-based FPs from different organisms is in the range of 35 to 50 %.

In most cases, the oligomeric state of the LOV-based FPs studied here has not been determined for the fluorescent protein but for the respective original LOV-domains that contain the cysteine residue involved in photoadduct formation. However, it can be assumed that the overall structure as well as the dimer interface regions of LOV-domains and their respective fluorescing variants is very similar. According to this assumption, all LOV-based FPs with bacterial origin form dimers, whereas the two LOV-based FPs derived from LOV2 domain of *Arabidopsis thaliana* phototropin 2 are monomeric proteins (Tab.1 and references therein). Nevertheless, until today no experimental artifacts related to the dimeric nature of LOV-based FPs (e.g. mislocation of fusion proteins) have been reported so far.

In a set of comparative studies, the extinction coefficients (ε) and the fluorescence quantum yields (Φ_F) were determined for all investigated LOV-based FPs (Tab. 1). Since in previous studies the extinction coefficient of free FMN was used for LOV-based FPs, we first measured the extinction coefficient of the LOV-FPs by comparing the absorption of the chromophore at 450 nm in the bound and unbound state (see materials and methods). This analysis revealed that the extinction coefficients of all tested LOV-based FPs only differ to a minor extent ranging from 13,900 $M^{-1}cm^{-1}$ (Pp1FbFP) to 15,100 $M^{-1}cm^{-1}$ (Pp2FbFP Q116V) with a mean value of approximately 14,300 $M^{-1}cm^{-1}$. Thus, the average extinction coefficient of LOV-based FPs is 17 % higher than that of the free chromophore FMN (12.200 $M^{-1}cm^{-1}$ [44]). In contrast, the fluorescence quantum yields vary considerably among the LOV-based FPs and can be almost twice as high as that of FMN (see below and Tab. 1).

Photochemical & Photobiological Science

RSCPublishing

ARTICLE

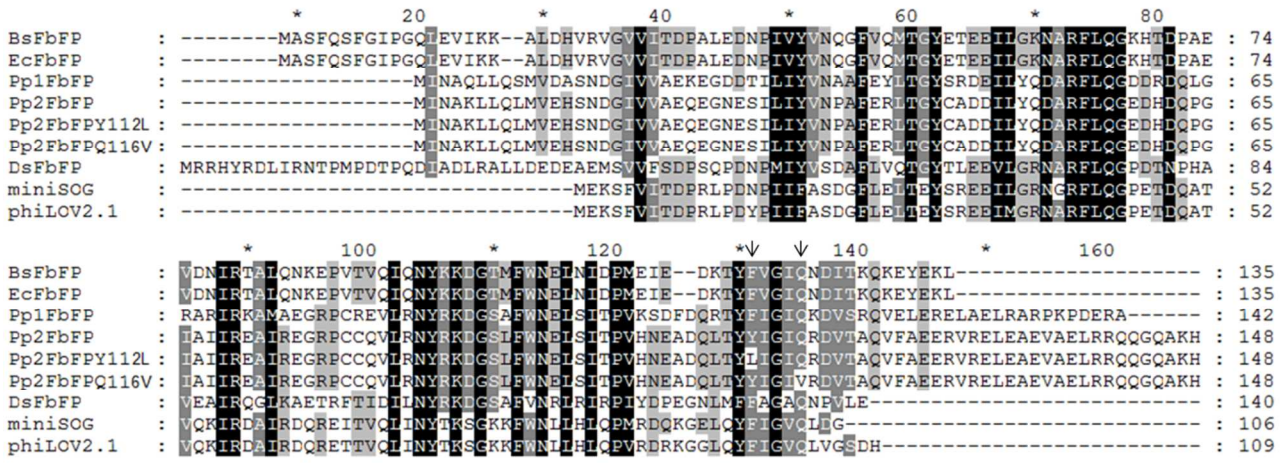

Fig. 1 Multiple sequence alignment of chosen LOV-based FPs. Homologous and similar residues are highlighted in black and gray, respectively. For BsFbFP, which still contains the effector domain at the C-terminal end, only the LOV-domain was used for the alignment. The numbers refer to the amino acid position of DsFbFP because it has the longest N-terminal sequence before the conserved LOV-domain. The arrows indicate the position of the Y112L and Q116V mutations in Pp2FbFP.

Tab. 1 Photophysical properties of LOV-based fluorescent proteins.

Name	Source organism	Molecular Mass (kDa)	Oligo-meric state	Absorption λ_{max} (nm)	Fluorescence λ_{max} (nm)	ε (M^{-1} cm^{-1})	Φ_F	Brightness (M^{-1} cm^{-1})	$\tau_{fl,\ ave}$ (ns)	$t_{bl,\ 50\%}$ (min)
BsFbFP	*B. subtilis*	28.7	dimer[a]	449	495	13,900 ± 400	0.39 ± 0.01	5420	5.68 ± 0.01	1.97 ± 0.05
EcFbFP	*B. subtilis*	15.1	dimer[a]	448	496	14,500 ± 200	0.44 ± 0.01	6380	5.70 ± 0.02	2.81 ± 0.10
Pp1FbFP	*P. putida*	16.3	dimer[b]	450	496	13,900 ± 500	0.27 ± 0.01	3750	3.90 ± 0.28	6.75 ± 0.83
Pp2FbFP	*P. putida*	16.3	dimer[c]	449	495	14,200 ± 50	0.22 ± 0.01	3120	3.17 ± 0.01	2.68 ± 0.19
Pp2FbFP Y112L	*P. putida*	16.3	dimer[c]	449	496	14,000 ± 50	0.30 ± 0.01	4200	4.56 ± 0.01	1.52 ± 0.09
Pp2FbFP Q116V	*P. putida*	16.3	dimer[c]	439	485	15,100 ± 350	0.26 ± 0.01	3930	3.53 ± 0.01	1.17 ± 0.04
DsFbFP	*D. shibae*	15.2	dimer[d]	449	498	14,300 ± 50	0.35 ± 0.01	5000	5.66 ± 0.01	0.35 ± 0.03
miniSOG	*A.thaliana*	12.1	monomer[e]	447	497	14,200 ± 700	0.41 ± 0.01	5820	5.46 ± 0.01	2.85 ± 0.23
phiLOV2.1	*A.thaliana*	12.1	monomer[f]	450	497	n.d.	0.20 ± 0.01	n.d.	3.36 ± 0.06	12.97 ± 0.74
FMN		0.456		444	531	12,200[g]	0.25 ± 0.01	3050	4.38 ± 0.30	0.325 ± 0.04

ε (extinction coefficient), Φ_F (fluorescence quantum yield), $\tau_{fl,ave}$ (average fluorescence lifetime) and $t_{bl,50\%}$ (time for bleaching fluorescence intensity down to 50% of the initial value) given as mean values with the standard deviation determined from three independent measurements. Fluorescence brightness is specified as the product of the extinction coefficient and the fluorescence quantum yield of the respective LOV-based FP. The extinction coefficient as well as the fluorescence brightness of phiLOV2.1 could not be determined, because the protein aggregated at 95°C.

[a]BsFbFP, EcFbFP: [14, 49, 52]; [b]Pp1FbFP: [14, 43, 51]; [c]Pp2FbFP and variants: [43, 53]; [d]DsFbFP: [42]; [e]miniSOG: [12]; [f]phiLOV: [10, 14]; [g]FMN: [44]

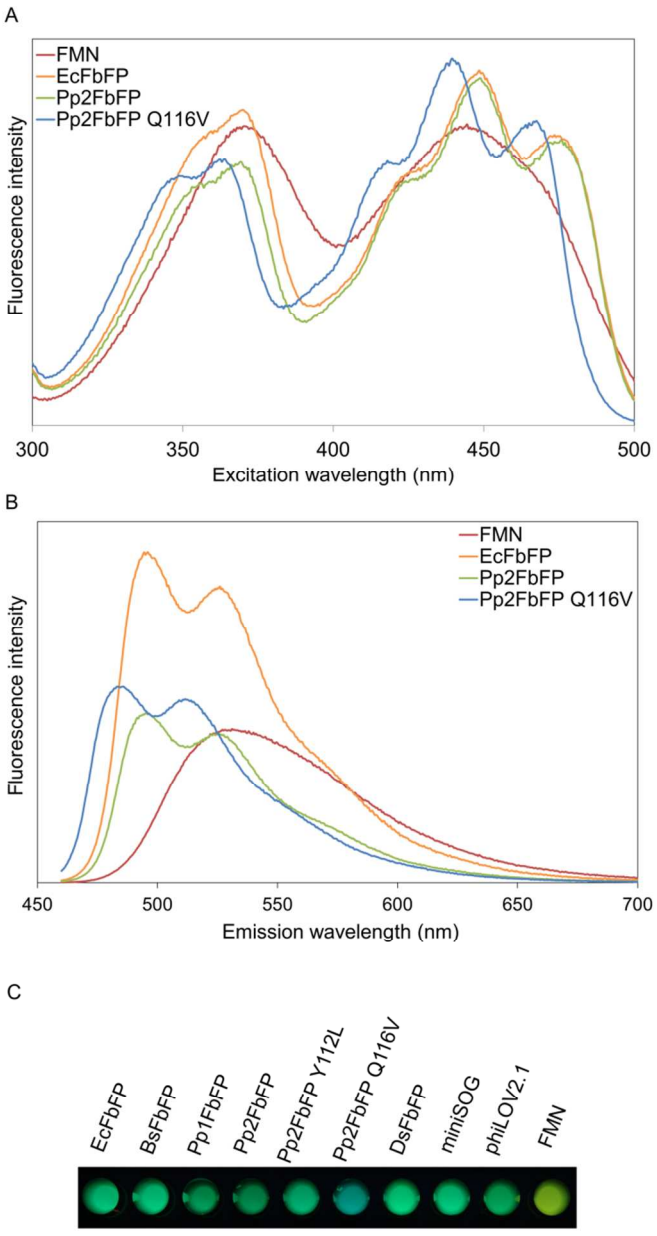

Fig. 2 Excitation and emission spectra of LOV-based FPs and FMN. (A) Excitation spectra of purified FPs and FMN. Fluorescence emission at 520 nm was recorded and all values were normalized to the extinction coefficient of the protein or FMN. (B) Fluorescence emission spectra. All spectra were normalized to the absorption of the samples at the excitation wavelength (450 nm) so that the integrals of the spectra are proportional to the quantum yield of the respective proteins. With the exception of Pp2FbFP Q116V with its blue-shifted excitation and emission spectrum, the spectra of all LOV-based FPs investigated here are very similar (EcFbFP and Pp2FbFP are shown exemplarily) and differ only in height due to their different fluorescence quantum yields. The complete comparison of all LOV-based FP excitation and emission spectra is shown in supplementary figures 1 and 2, respectively. (C) Comparison of fluorescence color. Samples of equal absorption were placed in a microtiter plate and illuminated with UV-light (λ = 365 nm). While FMN shows a yellow-green fluorescence, LOV-based FPs exhibit a cyan-green fluorescence. The 10 nm blue-shift of Pp2FbFP Q116V fluorescence is sufficient to visually distinguish the color variant from common LOV-based FPs.

Due to the invariable extinction coefficient the fluorescence quantum yield (Φ_F) represents one of the most important qualities of LOV-based FPs with respect to their applicability as fluorescent labels. so far, Φ_F values were reported only for miniSOG (0.37 [12]), EcFbFP (0.39 [8]) and Pp2FbFP (0.17 [8]). In a recent study that compared three LOV-based FPs [14], two of the fluorescence quantum yields differed significantly from the ones in the original publications (iLOV: 0.34 instead of 0.44 [9]); EcFbFP: 0.34 instead of 0.39 [8]) while the third was identical (Pp2FbFP: 0.17 [8]).

It is a long known phenomenon for photoreceptor proteins as well as for GFP-like fluorescent proteins that certain photophysical properties like the photoreaction or fluorescence quantum yields show a high variability when measured and published over the years by different groups. This is an inherent problem for these photoproteins when compared to simple organic fluorescent dyes that can be synthesized and supplied with very high purity grade. Generally, these photoproteins are heterologously expressed which might affect their correct folding. Furthermore, they have to incorporate or form an endogenous chromophore molecule. These different steps may vary in their effectiveness or quality and lead to differences in the estimated and published quantum yields that can be remarkable e.g. for. GFP-like FPs see [54].

An important motivation of this study was to compare the photophysical properties and especially the fluorescence quantum yields under identical experimental conditions (e.g. using the same bacterial strains, purification methods, identical solutions and fluorescence spectroscopy equipment). In particular, we have used a fluorescence spectrophotometer that corrects for wavelength-dependent detector sensitivity, as well as lamp emission intensity in conjunction with an integrating sphere, which allows for the absolute determination of Φ_F without a reference standard. The commonly applied comparative method for Φ_F determination was used in all earlier studies on LOV-based FPs. However, the comparison of the fluorescence spectra of a fluorescent dye with known Φ_F (standard) and that of the fluorophore under investigation is error prone, since it requires proper correction for differences in absorption and fluorescence spectra.

The instrumental setup with the integrating sphere that has been used here was first verified by measuring the quantum yield (ΦF) of the well characterized fluorescent dye fluorescein in 0.1M NaOH(aq) (published ΦF between 0.91 and 0.95 [55]; measured ΦF = 0.931 ± 0.008), as well as riboflavin (published Φ_F = 0.26 [56]; measured Φ_F = 0.247 ± 0.007) and flavin adenine dinucleotide (published Φ_F = 0.03 [57]; measured Φ_F = 0.032 ± 0.0004). All three determined fluorescence quantum yields (low, intermediate and high) are in excellent agreement with the literature data and prove the high accuracy of measurements with an integrating sphere. For this reason we are convinced that the Φ_F values published here represent a data set that describes the fluorescence quantum yield of LOV-based FPs correctly and unambiguously.

It should also be mentioned that we were unable to find a publication that actually determined the fluorescence quantum yield of FMN. Van den Berg and coworkers [58] cite a Φ_F of 0.26 for FMN with reference to [59], were FMN is not mentioned whereas Holzer and colleagues [60] refer to a Φ_F of 0.26 with reference to [56], where the Φ_F of riboflavin, but not FMN was determined. In this study we measured Φ_F = 0.246 ± 0.002 for FMN, which is identical to the value we measured for riboflavin (Φ_F = 0.247 ± 0.007). This was expected, considering

that FMN only differs from riboflavin by the presence of a phosphate group instead of a hydroxyl group at the end of the ribityl side chain. This value can also be used as a standard in future investigations when the fluorescence quantum yields of LOV-based FPs shall be determined with the comparative method.

The fluorescence quantum yields described in Tab. 1 are all slightly higher than the previously published values, which we believe is due to differences in protein preparations as well as in the used methods and instruments. The highest Φ_F obtained so far are those from EcFbFP ($\Phi_F = 0.44$) and iLOV, which was also reported to be 0.44 [9]. DsFbFP also shows a quite high Φ_F (0.35), while the other FbFP derivatives exhibit ΦF values ranging from 0.22 to 0.3.

It should be noted that for iLOV extensive directed evolution experiments were applied to increase the Φ_F of the original LOV domain whereas EcFbFP contains no further mutations. In this context it is worth mentioning that all attempts to increase the Φ_F of EcFbFP by directed evolution approaches have been unsuccessful so far (data not shown). In contrast, in case of Pp2FbFP the residue Y112 was identified as a key amino acid for influencing the quantum yield. A saturation mutagenesis of this position in Pp2FbFP resulted in the generation of several variants that exhibited a brighter *in vivo* fluorescence (data not shown). The brightest Pp2FbFP derivative was characterized in detail and showed a significantly increased quantum yield of 0.3 and carried a leucine at position 112. In contrast, all other LOV-based FPs carry a conserved phenylalanine at this position (Fig. 1) and – except for phiLOV2.1 – have a higher fluorescence quantum yield than Pp2FbFP.

It is usually desirable to have proteins with a high Φ_F, however, fluorescence brightness may subsequently be lost again during the optimization process for other properties such as photostability. This observation has been made in the case of phiLOV2.1 ($\Phi_F = 0.2$, Tab, 1), which is reported to be far more photostable than iLOV ($\Phi_F = 0.44$) [10].

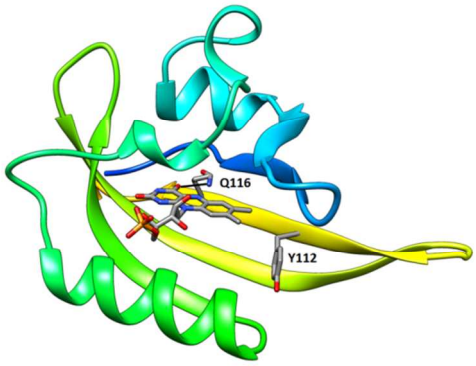

Fig. 3 Modeled structure of the Pp2FbFP core domain. The model shows the positions of the amino acids Y112 and Q116, which are mutated in the two variants described here. Y112 is located approximately 5 Å from the isoalloxazine ring and appears to have a fluorescence quenching effect, which can be abolished by exchanging this amino acid by a hydrophobic amino acid like phenylalanine or leucine. According to the model, Q116 can form a hydrogen bond with the FMN at a distance of about 3.1 Å. It is assumed that the absence of this hydrogen bond in the Pp2FbFP variant Q116V is responsible for the spectral shift.

Since the photostability of fluorescent reporter proteins is an important issue for imaging approaches, we further compared light-mediated bleaching of the LOV-based FP fluorescence. According to the results of our photobleaching assay (Table 1) it is obvious that photostability of LOV-based FPs is highly variable with bleaching half-times $t_{1/2}$ ranging from 0.35 (DsFbFP) to 13 minutes (phiLOV2.1). Remarkably, even the two derivatives of Pp2FbFP that only differ in a single amino acid residue exhibited a decrease in photostability by a factor of up to 2.3. The photobleaching of iLOV and its enhanced derivative phiLOV2.1 has been shown to be reversible *in vivo* [9, 10]. However, in our *in vitro* experiments photobleaching of all analyzed LOV-based FPs, including phiLOV2.1, was irreversible (data not shown), indicating that one or more yet unknown cellular components are required for the recovery of fluorescence after bleaching. For phiLOV2.1, which has been engineered towards higher photostability by several rounds of directed evolution, it has been proposed that the increased photostability is a result of a more rigid packing of the chromophore and especially its ribityl chain in the protein [10]. FMN itself has a high quantum yield for the generation of singlet oxygen and other reactive oxygen species under illumination [12, 61, 62], which are likely to play a major role in irreversible photobleaching.

In addition to brightness and photostability, we also compared the spectral characteristics of the LOV-based FPs. As expected, all tested LOV-based FPs exhibit the characteristic excitation spectra of LOV proteins with a prominent three band feature in the blue spectral region and the maximum near 450 nm (Fig. 2A, where the excitation spectrum of Pp2FbFP is exemplarily shown). An exception is the Pp2FbFP variant Q116V that exhibits a similar spectral shape but with a 10 nm blue-shifted maximum (Fig. 2A). The emission spectra of all LOV-based FPs are again spectrally very similar with a specific fluorescence maximum around 495 nm and a prominent vibrational transition in the range of 525 – 540 nm (see Figure 2B). Again, the Q116V variant of Pp2FbFP shows a spectrum similar to the other LOV-based FPs but is significantly blue-shifted (Figure 2B). Figure 2C illustrates the significant differences between the spectral properties of free FMN and FMN bound to LOV-based FPs. While free FMN shows a yellow-green fluorescence with its emission maximum at 531 nm, the LOV-based FPs show a cyan-green fluorescence. The 10 nm blue-shift of Pp2FbFP Q116V is sufficient to visually distinguish the protein from the other LOV-based FPs.

This blue-shift has also been described for other LOV-domains, where the glutamine at the respective position was exchanged [10, 63, 64] and it is assumed that this spectral shift is caused by the absence of the hydrogen bond formed between the glutamine and FMN (the position of Q116 within the proposed Pp2FbFP structure is shown in Fig. 3). Due to the conservation of this spectral change, we believe that this spectral shift can also be introduced to other LOV-based FPs. Further spectral shifts to allow for dual color imaging would be very useful and are routinely included in our ongoing screening of new variants.

The fluorescence intensity decays as a function of time of the LOV-based FPs show remarkable variability with average fluorescence lifetimes between 3.17 ns (Pp2FbFP) and 5.70 ns (EcFbFP) (Tab. 1). Figure 4 depicts a short, a long as well as an intermediate fluorescence intensity decay. The decays of the LOV-based FPs are either truly monoexponential (BsFbFP, EcFbFP, miniSOG) or biexponential (DsFbFP, Pp1FbFP, Pp2FbFP and its variants, phiLOV2.1) (see supplementary table 1). BsFbFP, EcFbFP, DsFbFP and miniSOG have considerably longer average fluorescence lifetimes (> 5 ns) compared to free FMN in aqueous solutions. More importantly, these lifetimes are much longer than those of FPs of the GFP-family, which are typically 1.5 to 3 ns but not longer than 4 ns [65, 66]. This renders

LOV-based FPs useful as partners for Förster resonance energy transfer (FRET) applications (e.g. utilization as fluorescent donor domains within genetically encoded FRET-based sensors, or analyses of protein-protein interactions), where FRET is detected with the help of fluorescence lifetime imaging (FLIM) *via* the measurement of the donor fluorescence lifetime [67]. The longer the unaffected fluorescence lifetime of the donor FP is, the better the occurrence of FRET is observable due to a more sensitive detection of subtle fluorescence lifetime changes.

In this respect, it is interesting to note, that the slower component of DsFbFPs bi-exponential fluorescence decay is very long (6.6 ns). By using directed evolution, it thus might be possible to generate a DsFbFP mutant with a mono-exponential fluorescence decay and a fluorescence lifetime near 6.5 ns. Such a variant may also have a considerably enhanced fluorescence quantum yield. A similar optimization has been performed by the Gadella lab for the cyan fluorescent protein, finally creating mTurquoise2 with largely increased fluorescence quantum yield and lifetime [65].

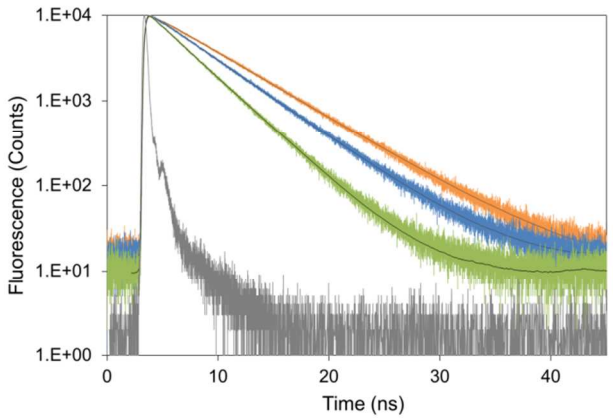

Fig. 4 Fluorescence lifetime spectroscopy of selected FbFPs. Experimental and fitted fluorescence decay curves (excitation: 440 nm, detection 495 nm) of EcFbFP (orange curve), Pp2FbFP Y112L (blue curve), Pp2FbFP (green curve), and the instrument response function (gray curve) are shown (excitation and detection: 440 nm). Experimental data are fitted with a mono-exponential functions in case of EcFbFP, and bi-exponential functions in case of Pp2FbFP and Pp2FbFP Y112L. The χ^2 values for the fluorescence intensity decays EcFbFP, Pp2FbFP and Pp2FbFP Y112L are 1.3, 1.0 and 1.0, respectively. The fluorescence decay curves of all characterized LOV-based FPs are shown in supplementary figure 3.

Besides FRET, FLIM represents another exciting application of LOV-based FPs with different fluorescence lifetimes. FLIM allows to distinguish between different fluorophores that are spectrally identical or similar but have a different fluorescence lifetime. By fusing fluorescent proteins with such properties to different proteins of interest one can determine the distribution of two or three proteins in cells in a single FLIM image. For this proposed experimental setup, only one excitation wavelength and one fluorescence detection channel is used, thereby circumventing potential limitations caused by chromatic aberration. Similarly, different bacteria expressing suitable FPs can be distinguished in this elegant way. For GFP-like FPs this has already been demonstrated [68, 69]. The here reported fluorescence lifetimes of LOV-based FPs, which are much longer than those of typical GFP-like FPs, as well as the independence of molecular oxygen make LOV-based FPs promising candidates for such applications.

For the two Pp2FbFP variants, the enhanced fluorescence quantum yield is accompanied by a significantly longer fluorescence lifetime. Both mutants and Pp2FbFP itself have bi-exponential fluorescence decays, where the short decay component (0.5 to 1 ns fluorescence lifetime) can be attributed to efficient quenching of the FMN fluorescence by several nearby amino acids. In the case of the replacement of glutamine 116 by valine only the relative amplitude of the short decay component is lowered compared to Pp2FbFP (data not shown) but the two fluorescence lifetimes are still unaffected. Nevertheless, the quenched component in Pp2FbFP cannot be attributed to a direct quenching of the FMN fluorescence by the hydrogen bonding of Q116 to FMN since this glutamine is also present in LOV-based FPs that have a strictly mono-exponential fluorescence decay behavior (i.e. EcFbFP, BsFbFP, miniSOG). On the other hand, for Pp2FbFP Y112L the fluorescence lifetime of the major decay component is significantly prolonged, while the shorter is reduced and again lower in amplitude. Tyrosine 112 seems to have not only a direct quenching effect, but obviously also indirectly changes the structure of the FMN chromophore pocket, thereby disfavoring the internal relaxation deactivation channel of the FMN's excited state. This leads to a higher fluorescence quantum yield and a longer fluorescence lifetime. In general, we found an approximate proportionality between the fluorescence quantum yield and the average fluorescence lifetime for the nine investigated LOV-based FPs.

Conclusions

The photophysical properties of nine LOV-based FPs investigated here prove them to be valuable candidates for protein localization and protein-protein interaction studies, especially under conditions of limited molecular oxygen supply. In addition, some of them are promising candidates to replace GFP-like FPs in genetically-encoded FRET-based sensors as well as in FRET applications with detection *via* the donor fluorescence lifetime due to their extraordinary long fluorescence lifetimes. The data presented in this study can provide a reasonable starting point for future optimization regimen of LOV-based FPs. Knowledge of the important photophysical properties of the most often used LOV-based FPs reported here will enable scientists to choose the best reporter protein for their specific purposes.

Acknowledgements

We thank the Ministry of Innovation, Science and Research of North Rhine-Westphalia and Heinrich-Heine-University Düsseldorf for the scholarship within the CLIB-Graduate Cluster Industrial Biotechnology. This work was also partially supported by grants from Federal Ministry of Education and Research (OptoSys, FKZ 031A16). G. Casini's stay in the ICS-4 was possible due to the support of the Commission of the European Communities within the framework of the LLP Erasmus Program. The content of the publication is the sole responsibility of the publisher and the European Commission is not liable for any use that may be made of the information. The authors also thank Dr. Sascha Hausmann from evocatal GmbH (Germany) for his kind support in creating some of the Pp2FbFP variants.

Notes and references

[a] *Institute of Molecular Enzyme Technology, Heinrich-Heine-University Düsseldorf, Forschungszentrum Jülich, 52425 Jülich, Germany, Fax: +49 2461 612490; Tel: +49 2461 614173; E-mail: t.drepper@fz-juelich.de*

[b] *Institute of Complex Systems 4 (ICS-4, Cellular Biophysics), Forschungszentrum Jülich, 52425 Jülich, Germany, Fax: +49 2461 614216; Tel: +49 2461 618068; E-mail: t.gensch@fz-juelich.de*

1. R. N. Day and M. W. Davidson, *Chem Soc Rev*, 2009, **38**, 2887-2921.
2. D. M. Chudakov, M. V. Matz, S. Lukyanov and K. A. Lukyanov, *Physiol Rev*, 2010, **90**, 1103-1163.
3. R. Y. Tsien, *Angewandte Chemie*, 2009, **48**, 5612-5626.
4. P. Dedecker, F. C. De Schryver and J. Hofkens, *Journal of the American Chemical Society*, 2013, **135**, 2387-2402.
5. R. H. Newman, M. D. Fosbrink and J. Zhang, *Chem Rev*, 2011, **111**, 3614-3666.
6. N. C. Shaner, P. A. Steinbach and R. Y. Tsien, *Nat Methods*, 2005, **2**, 905-909.
7. S. J. Remington, *Curr Opin Struct Biol*, 2006, **16**, 714-721.
8. T. Drepper, T. Eggert, F. Circolone, A. Heck, U. Krauss, J. K. Guterl, M. Wendorff, A. Losi, W. Gärtner and K. E. Jaeger, *Nat Biotechnol*, 2007, **25**, 443-445.
9. S. Chapman, C. Faulkner, E. Kaiserli, C. Garcia-Mata, E. I. Savenkov, A. G. Roberts, K. J. Oparka and J. M. Christie, *Proc Natl Acad Sci U S A*, 2008, **105**, 20038-20043.
10. J. M. Christie, K. Hitomi, A. S. Arvai, K. A. Hartfield, M. Mettlen, A. J. Pratt, J. A. Tainer and E. D. Getzoff, *J Biol Chem*, 2012.
11. T. Drepper, T. Gensch and M. Pohl, *Photochemical & photobiological sciences : Official journal of the European Photochemistry Association and the European Society for Photobiology*, 2013, **12**, 1125-1134.
12. X. Shu, V. Lev-Ram, T. J. Deerinck, Y. Qi, E. B. Ramko, M. W. Davidson, Y. Jin, M. H. Ellisman and R. Y. Tsien, *PLoS Biol*, 2011, **9**, e1001041.
13. J. Walter, S. Hausmann, T. Drepper, M. Puls, T. Eggert and M. Dihné, *PLoS One*, 2012, **7**, e43921.
14. A. Mukherjee, J. Walker, K. B. Weyant and C. M. Schroeder, *PloS one*, 2013, **8**, e64753.
15. J. F. Ernst and D. Tielker, *Cell Microbiol*, 2009, **11**, 183-190.
16. D. J. Hassett, M. D. Sutton, M. J. Schurr, A. B. Herr, C. C. Caldwell and J. O. Matu, *Trends Microbiol*, 2009, **17**, 130-138.
17. T. R. Rustad, A. M. Sherrid, K. J. Minch and D. R. Sherman, *Cell Microbiol*, 2009, **11**, 1151-1159.
18. M. Schobert and P. Tielen, *Future Microbiol*, 2010, **5**, 603-621.
19. H. K. Eltzschig and P. Carmeliet, *N Engl J Med*, 2011, **364**, 656-665.
20. J. M. Brown, *Methods in enzymology*, 2007, **435**, 297-321.
21. X. Lu and Y. Kang, *Clin Cancer Res*, 2010, **16**, 5928-5935.
22. J. D. Coates and R. T. Anderson, *Trends in biotechnology*, 2000, **18**, 408-412.
23. D. Karakashev, A. B. Thomsen and I. Angelidaki, *Biotechnol Lett*, 2007, **29**, 1005-1012.
24. F. E. Loffler and E. A. Edwards, *Current opinion in biotechnology*, 2006, **17**, 274-284.
25. J. B. McKinlay and C. S. Harwood, *Current opinion in biotechnology*, 2010, **21**, 244-251.
26. D. Tielker, I. Eichhof, K. E. Jaeger and J. F. Ernst, *Eukaryot Cell*, 2009, **8**, 913-915.
27. C. H. Choi, J. V. Deguzman, R. J. Lamont and Ö. Yilmaz, *PLoS One*, 2011, **6**, e18499.
28. L. A. Lobo, C. J. Smith and E. R. Rocha, *FEMS Microbiol Lett*, 2011.
29. G. Z. Cui, W. Hong, J. Zhang, W. L. Li, Y. Feng, Y. J. Liu and Q. Cui, *J Microbiol Methods*, 2012, **89**, 201-208.
30. J. Potzkei, M. Kunze, T. Drepper, T. Gensch, K. E. Jaeger and J. Büchs, *BMC Biol*, 2012, **10**, 28.
31. C. Zhang, M. S. Liu and X. H. Xing, *Applied microbiology and biotechnology*, 2009, **84**, 511-517.
32. J. Seago, N. Juleff, K. Moffat, S. Berryman, J. M. Christie, B. Charleston and T. Jackson, *J Gen Virol*, 2013, **94**, 1517-1527.
33. T. Drepper, R. Huber, A. Heck, F. Circolone, A. K. Hillmer, J. Büchs and K. E. Jaeger, *Appl Environ Microbiol*, 2010, **76**, 5990-5994.
34. S. M. Kitson, W. Mullen, R. J. Cogdell, R. M. Bill and N. J. Fraser, *Methods*, 2011, **55**, 287-292.
35. J. A. Gawthorne, L. E. Reddick, S. N. Akpunarlieva, K. S. Beckham, J. M. Christie, N. M. Alto, M. Gabrielsen and A. J. Roe, *PloS one*, 2012, **7**, e52962.
36. K. E. Scholz, D. Okrob, B. Kopka, A. Grünberger, M. Pohl, K. E. Jaeger and U. Krauss, *Applied and environmental microbiology*, 2012, **78**, 5025-5027.
37. K. E. Scholz, B. Kopka, A. Wirtz, M. Pohl, K. E. Jaeger and U. Krauss, *Applied and environmental microbiology*, 2013, **79**, 4727-4733.
38. A. Mukherjee, K. B. Weyant, J. Walker and C. M. Schroeder, *Journal of Biological Engineering*, 2012, **6**, 20.
39. X. Song, Y. Wang, Z. Shu, J. Hong, T. Li and L. Yao, *PLoS Comput Biol*, 2013, **9**, e1003129.
40. D. Hanahan, *J Mol Biol*, 1983, **166**, 557-580.
41. N. Katzke, S. Arvani, R. Bergmann, F. Circolone, A. Markert, V. Svensson, K. E. Jaeger, A. Heck and T. Drepper, *Protein Expr Purif*, 2010, **69**, 137-146.
42. F. Circolone, J. Granzin, A. Stadler, U. Krauss, T. Drepper, S. Endres, E. Knieps-Grünhagen, A. Wirtz, A. Cousin, P. Tielen, D. Willbold, K. E. Jaeger and R. Batra-Safferling, **in preparation**.
43. K. Jentzsch, A. Wirtz, F. Circolone, T. Drepper, A. Losi, W. Gärtner, K. E. Jaeger and U. Krauss, *Biochemistry*, 2009, **48**, 10321-10333.
44. L. G. Whitby, *Biochem J*, 1953, **54**, 437-442.
45. A. Geiger, L. Russo, T. Gensch, T. Thestrup, S. Becker, K. P. Hopfner, C. Griesinger, G. Witte and O. Griesbeck, *Biophysical journal*, 2012, **102**, 2401-2410.
46. W. Becker, *Advanced Time-Correlated Single Photon Counting Techniques*, Springer Berlin Heidelberg, 2005.
47. F. Sievers, A. Wilm, D. Dineen, T. J. Gibson, K. Karplus, W. Li, R. Lopez, H. McWilliam, M. Remmert, J. Söding, J. D. Thompson and D. G. Higgins, *Mol Syst Biol*, 2011, **7**, 539.
48. A. Sali and T. L. Blundell, *J Mol Biol*, 1993, **234**, 779-815.
49. A. Möglich and K. Moffat, *J Mol Biol*, 2007, **373**, 112-126.

50. E. F. Pettersen, T. D. Goddard, C. C. Huang, G. S. Couch, D. M. Greenblatt, E. C. Meng and T. E. Ferrin, *J Comput Chem*, 2004, **25**, 1605-1612.
51. F. Circolone, J. Granzin, K. Jentzsch, T. Drepper, K. E. Jaeger, D. Willbold, U. Krauss and R. Batra-Safferling, *J Mol Biol*, 2012.
52. C. Engelhard, S. Raffelberg, Y. Tang, R. P. Diensthuber, A. Moglich, A. Losi, W. Gärtner and R. Bittl, *Photochemical & photobiological sciences : Official journal of the European Photochemistry Association and the European Society for Photobiology*, 2013.
53. U. Krauss, A. Losi, W. Gärtner, K. E. Jaeger and T. Eggert, *Phys Chem Chem Phys*, 2005, **7**, 2804-2811.
54. M. Zimmer, *Chem Rev*, 2002, **102**, 759-781.
55. A. M. Brouwer, *Pure and Applied Chemistry*, 2011, **83**, 2213-2228.
56. G. Weber and F. W. J. Teale, *Transactions of the Faraday Society*, 1957, **53**, 646-655.
57. P. Wahl, J. C. Auchet, A. J. Visser and F. Müller, *FEBS letters*, 1974, **44**, 67-70.
58. P. A. van den Berg, J. Widengren, M. A. Hink, R. Rigler and A. J. Visser, *Spectrochim Acta A Mol Biomol Spectrosc*, 2001, **57**, 2135-2144.
59. G. Weber, *The Biochemical journal*, 1950, **47**, 114-121.
60. W. Holzer, A. Penzkofer, M. Fuhrmann and P. Hegemann, *Photochemistry and photobiology*, 2002, **75**, 479-487.
61. R. Ruiz-Gonzalez, A. L. Cortajarena, S. H. Mejias, M. Agut, S. Nonell and C. Flors, *Journal of the American Chemical Society*, 2013, **135**, 9564-9567.
62. F. M. Pimenta, R. L. Jensen, T. Breitenbach, M. Etzerodt and P. R. Ogilby, *Photochemistry and photobiology*, 2013, **89**, 1116-1126.
63. D. Nozaki, T. Iwata, T. Ishikawa, T. Todo, S. Tokutomi and H. Kandori, *Biochemistry*, 2004, **43**, 8373-8379.
64. M. A. Jones, K. A. Feeney, S. M. Kelly and J. M. Christie, *The Journal of biological chemistry*, 2007, **282**, 6405-6414.
65. J. Goedhart, D. von Stetten, M. Noirclerc-Savoye, M. Lelimousin, L. Joosen, M. A. Hink, L. van Weeren, T. W. Gadella, Jr. and A. Royant, *Nat Commun*, 2012, **3**, 751.
66. G. Jung, A. Brockhinke, T. Gensch, B. Hötzer, S. Schwedler and S. K. Veettil, *Fluorescent Proteins I. From Understanding to Design*, Springer Berlin Heidelberg, 2012.
67. H. Wallrabe and A. Periasamy, *Current opinion in biotechnology*, 2005, **16**, 19-27.
68. R. Pepperkok, A. Squire, S. Geley and P. I. Bastiaens, *Current biology : CB*, 1999, **9**, 269-272.
69. A. W. Scruggs, C. L. Flores, R. Wachter and N. W. Woodbury, *Biochemistry*, 2005, **44**, 13377-13384.

GRAPHICAL ABSTRACT

Manuscript ID PP-ART-12-2013-050414
" The photophysics of LOV-based fluorescent proteins – new tools for cell biology " authored by M. Wingen, J. Potzkei, S. Endres, G. Casini, C. Rupprecht, U. Krauss, K.-E. Jaeger, T. Drepper, and T. Gensch

In this study the excitation and emission spectra, the extinction coefficient, the fluorescence quantum yield, the average fluorescence lifetime and the photostability of selected fluorescent proteins that are based on blue-light photoreceptors derived from plants and bacteria are comparatively determined. This comprehensive characterization helps to apply this novel group of fluorescent proteins for analytic methods as well as imaging approaches.